7-22-2021

Raman Spectroscopy Reveals High Phloem Sugar Content in Leaves of Canopy Red Oak Trees

Jess T. Gersony
Harvard University, jgersony@smith.edu

Arthur McClelland
Harvard University

N Michele Holbrook
Harvard University

New
Phytologist

Methods

Raman spectroscopy reveals high phloem sugar content in leaves of canopy red oak trees

Jess T. Gersony[1] ![ORCID], Arthur McClelland[2] ![ORCID] and N. Michele Holbrook[1] ![ORCID]

[1]Department of Organismic and Evolutionary Biology, Harvard University, Cambridge, MA 02138, USA; [2]Center for Nanoscale Systems, Harvard University, Cambridge, MA 02138, USA

Author for correspondence:
Jess T. Gersony
Email: Jtgersony@gmail.com

Summary

• A robust understanding of phloem functioning in tall trees evades us because current methods for collecting phloem sap do not lend themselves to measuring actively photosynthesizing canopy leaves.

• We show that Raman spectroscopy can be used as a quantitative tool to assess sucrose concentration in leaf samples. Specifically, we found that Raman spectroscopy can predict physiologically relevant sucrose concentrations (adjusted R^2 of 0.9) in frozen leaf extract spiked with sucrose.

• We then apply this method to estimate sieve element sucrose concentration in rapidly frozen petioles of canopy red oak (*Quercus rubra*) trees and found that sucrose concentrations are > 1100 mM at midday and midnight. This concentration is predicted to generate a sieve element turgor pressure high enough to generate bulk flow through the phloem, but is potentially too high to allow for sucrose diffusion from photosynthetic cells.

• Our findings support the Münch hypothesis for phloem transport once the carbon is in the phloem and challenge the passive-loading hypothesis for carbon movement into the phloem for red oak. This study provides the first ~*in-situ* (frozen in the functioning state) source sieve element sucrose concentration characterization in any plant, opening a new avenue for investigation of phloem functioning.

Introduction

Phloem functioning influences important ecosystem processes, from carbon sequestration to drought-induced tree mortality (McDowell *et al.*, 2013; Nikinmaa *et al.*, 2013; Sevanto *et al.*, 2014). The movement of carbon out of the leaf has been proposed as a driver of assimilation (Nikinmaa *et al.*, 2013), and loss of phloem turgor is a key player in drought-induced tree death (Sevanto *et al.*, 2014). Yet despite this crucial role of the phloem, we lack a robust understanding of its physiology due to methodological limitations. Notably, the concentration of sucrose in the leaf sieve elements, hypothesized to be a critical parameter of whole-tree carbon movement and to dictate the amount of turgor in the phloem (Münch, 1930), is unknown for large trees. While saplings have been studied using aphid stylectomy (Öner-Sieben & Lohaus, 2014; Fink *et al.*, 2018), the primary methods used for sap collection are not suited for canopy measurements.

A majority of trees are thought to be symplastically passive loaders (hereafter referred to as 'passive') based on the species studied in the literature (Rennie & Turgeon, 2009; Liesche, 2017). For passive loaders, the concentration of sucrose in the leaf phloem links two hypotheses, one regarding the movement of carbon from sites of photosynthesis into the phloem (passive loading), and one regarding the movement of carbon from sources to sinks (osmotically driven pressure flow, also referred to as Münch flow). In passive loading, sucrose moves from mesophyll cells to the transport phloem (sieve element) via diffusion, which requires that the concentration of sucrose in the sieve elements is lower than that in the cytoplasm of mesophyll cells (Turgeon & Medville, 1998). At the same time osmotically driven pressure flow requires that the sucrose concentration in the sieve elements is high enough to draw water from the xylem and thereby generate sufficient positive pressure to drive bulk flow to the sink tissues (Munch, 1930). This is a challenge for canopy trees because they experience large decreases in water potential during the day (Fig. 1). While one solution would be to perform the majority of phloem loading and transport at night, in red oak, a reported passive loader (Rennie & Turgeon, 2009), the majority of carbon transport out of the leaf takes place during the day (Gersony *et al.*, 2020). The key question then follows: in red oak, is the source sieve element sucrose concentration high enough to support Münch flow, while being low enough to allow passive loading?

One potential complication to this question to note is that red oaks may not be exclusively passive loaders in that they may utilize a mixture of loading types, as has been suggested for other species (Slewinski *et al.*, 2013; Liesche, 2017). While there is evidence supporting the claim that red oak is a passive loader (Rennie & Turgeon, 2009), passive loading has been questioned for saplings of another oak species (*Quercus robur*) due to the sucrose
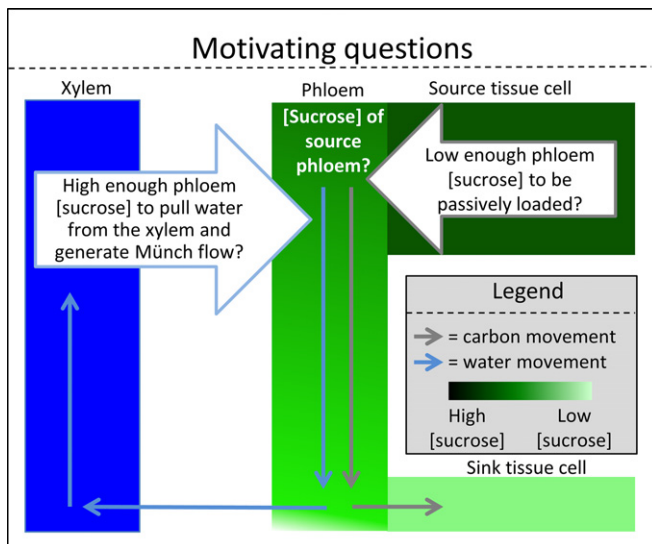
Fig. 1 Conceptual framework. The primary motivating question for this research is: what is the sucrose concentration in source phloem for *Quercus rubra*? The secondary motivating questions are as follows: first, is the concentration low enough to allow for passive loading to occur by diffusion from the mesophyll cell cytoplasm, and second, is the concentration high enough to draw in water from the xylem by osmosis during midday water stress, and subsequently generate enough pressure to drive phloem transport?

concentration of phloem sap in the leaves, obtained through aphid stylectomy, being substantially higher than measured cytoplasmic sucrose concentration (Öner-Sieben & Lohaus, 2014; Fink *et al.*, 2018). Saplings and mature trees were shown to have similar plasmodesmatal counts, indicating that they may have similar phloem loading strategies (Liesche *et al.*, 2019). Quantifying sieve element sucrose concentration in source phloem will shed important light on this topic.

To approach the question of whether the source sieve element sucrose concentration is high enough to support Münch flow, while being low enough to allow passive loading, we developed a new method that uses Raman spectroscopy to estimate sieve element sucrose concentration. Raman spectroscopy has been utilized to detect stress and infection in plants (Altangerel *et al.*, 2017; Mandrile *et al.*, 2019) but has never been used for quantifying cellular level sugar concentrations in plants. Fourier-transform infrared (FTIR) spectroscopy has recently been used to quantify sugar concentrations in plants; however, the spatial resolution was too large to resolve cellular level concentrations (Guendel *et al.*, 2018). Raman spectroscopy allows for the characterization of sucrose concentrations of sieve elements in leaves of mature, forest trees, furthering our understanding of phloem functioning for these ecologically important organisms.

Materials and Methods

Sample collection

Five mature (> 20 m) *Quercus rubra* L. (red oak) trees, an important species in North American temperate ecosystems (Taylor *et al.*, 2017), at Harvard Forest in Petersham, MA, USA (lat.

42.53°N, long. 72.19°W) were selected for study due to their south facing orientation into a clearing that provided access to fully illuminated leaves. Sampling occurred at midday and midnight on 30 July 2017. The date was selected due to there being minimal cloud cover (average and maximum photosynthetically active radiation (PAR) values were 954 and 1746 μmol m^{-2} s^{-1}, respectively). One leaf was sampled from each of the five trees at each time point for Raman analysis, and a neighboring leaf was sampled for water potential. The leaves for Raman analysis were immediately placed between two bags of dry ice to increase the rate of freezing and then transferred to a $-80°C$ freezer (within 30 h) until processing. Each leaf sampled for water potential was sealed into a humidified plastic bag, placed in an insulated box, and transported to the lab for measurement within 1 h.

Raman spectroscopy: sucrose calibration

We developed calibration curves by measuring Raman spectra of frozen droplets spanning a range of 34–1284 mM sucrose. Because Raman spectroscopy is sensitive to local chemistry, we used leaf extract as the solvent for our calibration solutions to mimic the chemical environment inside the phloem. While this is not an exact match for the local chemistry in the petiole, the similar shape of the Raman spectra from the phloem area of frozen petioles and the leaf extract standard samples argues that it is a reasonable approximation (spectra shown in Fig. 2). Leaf extract was collected by freezing and thawing leaves, then placing the lamina in an Eppendorf tube with a 0.22 μm pore cellulose acetate membrane containing filter (Costar 8161; Corning, Tewksbury, MA, USA). The tubes were then centrifuged for 10 min at 17 709 *g* to collect the extract (occasionally they were spun for an extra 5 min to obtain more liquid). A neighboring leaf was analyzed for sucrose content using the enzymatic-colorimetric assay method described by Gersony *et al.* (2020) to establish the baseline concentration in the extract (average of 34 mM). The extract was then spiked with 0–1250 mM of sucrose. We selected this range because it encompassed the findings in the literature (Jensen *et al.*, 2013; Öner-Sieben & Lohaus, 2014). All leaves used in determining the baseline sugar concentration for the calibration were collected from the same trees sampled for phloem concentration.

A Horiba (Irvine, CA, USA) Xplora confocal Raman microscope (785 nm laser, 30 s collection time, 5 μm depth below the surface) was used for all measurements. For each calibration solution, five 3-μl droplets were pipetted onto a metal block, which was then placed into a bowl of liquid nitrogen with *c.* 75% of the block submerged in liquid nitrogen. For each droplet, five Raman spectra were recorded at different locations. All measurements were made with the microscope enclosed in a plastic bag flooded with pure nitrogen gas to minimize ice formation. To account for instrument drift, two calibration curves were completed, one immediately before beginning the petiole measurements and the second one 2 wk later, immediately following the completion of the samples.

To predict sucrose concentration from Raman spectra, we used a genetic algorithm for variable selection to develop a partial least
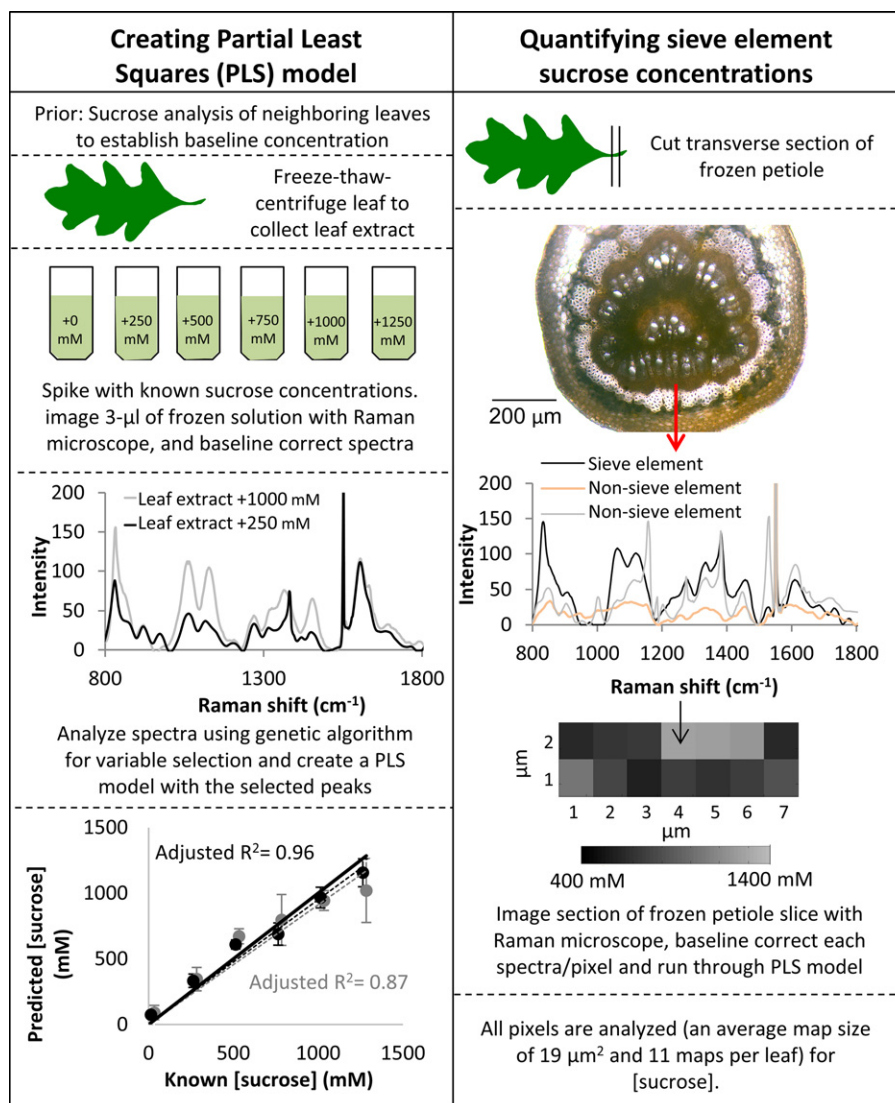
Fig. 2 Description of methods. To create the partial least squares (PLS) model, *Quercus rubra* leaf extract was spiked with known amounts of sucrose. Five 3 µl drops for each solution were frozen on a metal block and Raman spectra were collected five times from each drop. The peaks that correlated to the changes in sucrose concentration, chosen by a genetic algorithm for variable selection, were then used, along with the known concentrations of sucrose in the spiked extract, to create PLS models. One model was performed at the beginning of the sampling period (black) and another at the end of the sampling period (gray). Each point represents the average of the 5 3-µl-drops per solution, with the standard deviation between drops shown. To collect data on sieve elements, a frozen petiole slice (five petioles collected during the day and five during the night) was placed on a frozen block and measured with the Raman microscope. Multiple maps (average size = 19 µm²) of each petiole were made using a step size of 1 µm². The spectra from each map were then analyzed with the PLS model.

squares (PLS) regression for each calibration curve. Each spectrum was baseline corrected using the automatic Whitaker filter in SOLO+MIA (Eigenvector, Seattle, WA) to remove the contribution of fluorescence to the spectra. Then a genetic algorithm was used for variable selection in SOLO+MIA, using the default settings of population size (16), window width (1), % initial terms (30), penalty slope (0), maximum generations (100) and mutation rate (0.005), as well as five latent variables and three iterations of the cross-validation parameters to minimize overfitting (Leardi & González, 1998). The genetic algorithm selects which regions of the spectra most accurately predict sucrose concentrations. Based on these selected variables, a partial least squares regression model was created using the number of latent

variables suggested by SOLO+MIA (three and five for the first and second calibration curves, respectively) for optimal model performance relating the predicted vs known sucrose concentration of the leaf extract.

Raman spectroscopy: petiole sieve tube sucrose concentrations

Raman spectroscopy was used to estimate the sucrose concentration of sieve elements in petioles of leaves collected at midday and midnight. Frozen leaves were transferred from the −80°C freezer to the microscope on dry ice. Then, a transverse slice of the petiole was collected and secured with Tissuetek (Torrance,

CA, USA) to a metal block sitting in a bowl of liquid nitrogen on the microscope stage. Approximately 75% of the block was submerged in the liquid nitrogen throughout the imaging period. Raman maps (spatially explicit Raman spectra collection, average 19 μm^2) of the phloem area were collected over the course of 3–5 h, until an average of *c.* 200 spatially separated measurements were collected. The surface of the sample was determined by imaging the reflected focused excitation laser spot on a digital camera. Then the motorized focus was translated 5 μm below the surface of the sample to ensure quality spectra were collected despite slight unevenness in sample preparation and mounting. The microscope stage area was purged with nitrogen gas to minimize ice formation on the sample during data collection.

A light microscope was used to locate the phloem area. This was achieved by focusing on a large xylem vessel and moving the focus outward from the center of the stem, avoiding the ray parenchyma cells in the phloem area. The resolution of the light microscope was not high enough to generate comparable bright field images at the same scale as the Raman maps (1 μm^2 resolution). The phloem in the petiole of red oak is bounded by xylem on one side and by cortical fibers on the other, both of which have distinctly different Raman spectra from the phloem due to their thick and lignified cell walls (Gierlinger & Schwanninger, 2006). Raman spectra from a 400 nm^2 gaussian shaped area at the center of the 1 μm^2 area was then collected to confirm that signature Raman peaks for sucrose were present. The area was then mapped for as long as possible at 1 μm^2 resolution; once the sample moved or came out of focus, collection stopped and a new area was selected. Because of the high resolution of the data collection, microscopic movements of the sample often occurred when the liquid nitrogen in the bowl was refilled, thus limiting the map size to, on average, 19 μm^2 (Supporting Information Fig. S1). Occasionally, we did collect larger maps (42 μm^2); however, they necessarily involved adding liquid nitrogen to the bowl and thus may have lost spatial registration even though they remained in focus within the phloem area. The different areas to be mapped within the phloem area were selected based on what sections were within the same plane of focus (flat) and were distributed all around the petiole. Efforts to reduce bias between samples included performing all the measurements within 2 wk (to maintain user and instrument consistency), standardizing the amount of time for data collection (e.g. pixels measured) for each sample, and blinding the user to the identity (day vs night) of the sample they were measuring.

An average of 194 μm^2 per leaf were analyzed in the phloem area (*c.* 40 000 μm^2) of the petiole cross section for each leaf (*c.* 11 maps per petiole). Each spectrum was baseline corrected using the automatic Whitaker filter in SOLO+MIA to remove the contribution of fluorescence to the spectra. The spectra were then analyzed using the partial least squares regression models to predict the amount of sucrose in the pixel. For the first five leaves that were sampled, the calibration curve from the beginning of the experiment was used, while for the second five leaves that were sampled, the calibration curve from the end of the experiment was used. The standard deviation per map was 465 mM. Outliers (3.5% of all pixels) were excluded from each set of pixels

based on the interquartile range approach (Sokal & Rohlf, 1981; Asner *et al.*, 2003). Sieve element diameters for petioles and small stems are generally between 4–11 μm (Table S1), and our maps are therefore likely inside of single cells.

Turgor calculations

Balancing pressure measurements were made using a pressure chamber at each sampling time point (Soil Moisture Equipment, Santa Barbara, CA, USA). Water potential was calculated by accounting for gravity by adding 0.1 MPa to the balancing pressure measurements (*c.* 20 m tall trees). Sucrose concentration in the phloem was estimated, based on the literature, to be 88% of total osmolality (e.g. Pate, 1976; Jensen *et al.*, 2013). Turgor calculations were then made as the difference between the solute potential (calculated from the estimated osmolality, using the equation from Michel, 1972) and water potential.

Results

We found that Raman spectroscopy can be used as a quantitative tool for determining sucrose concentrations of plant samples (adjusted R^2 of *c.* 0.9; Fig. 2). We observed variation both within (Table S2) and between (presented as error bars in Fig. 2; Table S2) calibration droplets, which we attribute to differences in the angle of the frozen liquid meniscus influencing the spectra. For the first calibration curve the root mean square error of calibration (RMSEC) and the root mean square error of cross validation (RMSECV) (based on a venetian blinds cross validation strategy) values were 205.4 and 218.5 mM, respectively. For the second calibration curve, the RMSEC and RMSECV values were 238.4 and 277.3 mM. The RMSEC and RMSECV incorporate both the error between and within calibration drops.

Using Raman spectroscopy, we estimated sieve element sucrose concentrations. We found that the sucrose concentration in red oak source phloem area (inclusion of all collected spectra; 100% on the *x*-axis of Fig. 3a) at midday was 1065 mM (SE = 55 mM) and at midnight was 1110 mM (SE = 96 mM). This can also be considered a conservative estimate of sieve element sucrose concentration in that it represents the concentration of sucrose if every pixel we measured were made up of exclusively sieve elements. The literature suggests that, on an area basis, sieve elements comprise 35% of the phloem area (Table S3), that sieve elements have the highest osmolality of all the cells in the vascular bundle (in poplar leaf veins; Russin & Evert, 1985), and that the majority of phloem sap solutes are sucrose (Pate, 1976). Therefore, we used this information to guide our analysis of calculating sieve element sucrose concentration by considering the 35% of pixels with the highest sucrose concentration in each petiole to be sieve elements. Based on these considerations, we calculated that the sucrose concentration of sieve elements at midday was 1560 mM (SE = 101 mM) and 1600 mM (SE = 130 mM) at midnight (Fig. 3). We present histograms of the raw data from the maps as well as calculations for the lower 65% of pixels in Fig. S2 and Notes S1.
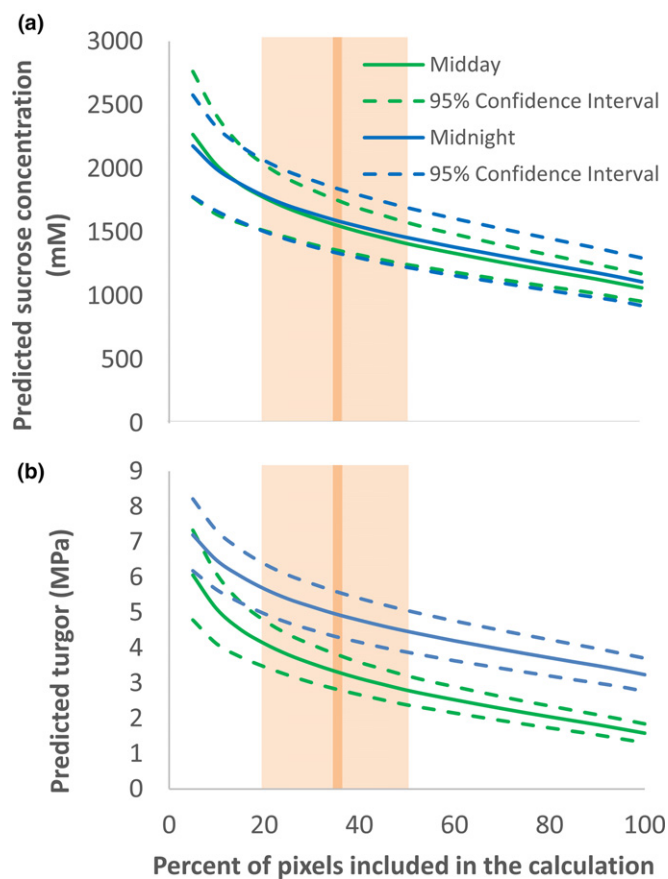
Fig. 3 Predicted sieve element sucrose concentration (a) and turgor pressure (b) in the petiole of large *Quercus rubra* trees. The solid lines represent the average of the five petioles from midday (green) and the five petioles from midnight (blue) (with the 95% confidence interval shown with dashed lines) based on the inclusion of 5–100% of pixels, starting with the pixels with the highest concentration. For example, the predicted sucrose concentration at 5% of the pixels included in the calculation is the average of the 5% of pixels with the highest concentration for each petiole, averaged across all five petioles. The orange bar highlights the predicted concentration based on the 35% of pixels with the highest concentration in each map, which, according to the literature, is the average percentage of sieve element area in the total phloem area. The lighter orange shaded areas show the 95% confidence interval for the 35% based on the data from the literature. In (b), the pressure is calculated based on water potential measurements and with the assumption that sucrose is 88% of total solutes in the phloem sap.

Using the predicted sucrose concentrations, we estimated the range of pressures generated in the sieve elements (depending on how many pixels were included in the calculation) to better understand whether the observed concentrations are high enough to support the Münch hypothesis. The lack of variation in estimated sucrose concentration between sampling times is surprising given the wide swing in leaf water potential (−0.3 MPa at midnight; −1.8 MPa at midday). Assuming a sucrose-to-total osmolality percentage for phloem sieve tubes from the literature (88%), and measuring xylem tension using a pressure bomb and accounting for gravity, we estimate, if 35% of the pixels are sieve elements, that the turgor generated in the sieve elements varies between 3.3 MPa (SE = 0.3 MPa) during

the middle of the day and 5 MPa (SE = 0.3 MPa) during the night (Fig. 3b). Using the conservative estimate for sieve element sucrose concentration of *c.*1100 mM, the estimated turgor generated in the sieve elements is 1.6 MPa (SE = 0.2 MPa) during the middle of the day and 3.2 MPa (SE = 0.2 MPa) during the evening.

Discussion

We have demonstrated that Raman spectroscopy can be used as a quantitative tool for measuring sucrose concentrations in sieve elements. This is both the first time leaf phloem sieve element sucrose concentrations have been characterized in mature trees, and the first time ~*in-situ* (frozen in the functioning state) characterizations of phloem sieve element sucrose concentration have been made for any plant. This methodological advancement will help further our understanding of fundamental phloem functioning, as well as how phloem functioning may change when trees are confronted by novel stressful conditions. Because the traditional methods for collecting phloem sap have their own uncertainties (Jensen *et al.*, 2013), the addition of a new method to our toolbox furthers our ability to assess our current understanding of phloem functioning.

It is important to note here that while this method shows considerable promise for investigating phloem functioning, the transferability of this approach to other species will need to be evaluated. Because species vary in the chemical composition of both their leaves (used for the calibration) and their phloem (in the collected spectra used to estimate phloem sap sugar concentrations), additional experiments are necessary to understand whether this approach will work in other species. For red oak, the calibration spectra and petiole spectra are similar (Fig. 2), with local peaks *c.* 830, 1060, 1120, 1270, 1330, 1380, 1450 and 1600 Raman shift (cm^{-1}), arguing for the validity of this method. However, because Raman is sensitive to local chemistry, it is unclear how secondary metabolites that are absent for red oak, but that may be present in other species, will influence the transferability of this method.

The range of sieve element sucrose concentrations estimated in this study (Fig. 3) is similar to what was found for sieve element sucrose concentrations in leaves of *Quercus robur* saplings (1015 mM; SD = 119) and by a xylem–phloem interaction model (1400 mM; Nikinmaa *et al.*, 2014), supporting the validity of this method. Interestingly, our findings are up to three times higher than previous measurements of phloem sucrose concentration in both red oak and other trees (all from non-source tissue or source tissue in saplings; Table S4), highlighting the potential variation within individuals and between species. Our findings are also hundreds of mM lower than the estimated concentration that would allow for optimal translocation of sugar given considerations of turgor and viscosity (Hölttä *et al.*, 2006). Our estimated concentrations are also higher than most concentrations observed for active loaders (Jensen *et al.*, 2013). Because the petiole is further downstream in the transport path than the sites of loading, we assume that the concentration in the loading zone must be at least this value.

The phloem pressures estimated here are comparable to what is reported for guard cells (4 MPa in *Vicia faba,* Raschke, 1979; and 5 MPa in *Chrysanthemum morifolium,* Bearce & Kohl, 1970), and are higher than those presented in a recent study of red oak (Savage *et al.*, 2017). However, in the recent red oak study phloem turgor was estimated from measurements of turgor in leaf mesophyll cells, an approach based on red oak being a passive loader. With the assumption that sink pressures are between 0.4 and 0.7 MPa, the pressures generated in the source of these red oak trees appear more than sufficient to drive Münch flow (a difference between source and sink pressure of 0.2 MPa is sufficient to drive flow; Savage *et al.*, 2017). This high pressure further suggests that, all else being equal, these trees could experience an additional drop of multiple MPa in leaf water potential before experiencing failures in phloem transport, underscoring the robustness of phloem transport. However, during drought stomata have a lower conductance and thus less assimilation, resulting in less sucrose to transport. Therefore, this turgor buffer should be viewed as a first-order approximation for drought scenarios and should be further validated with drought experiments.

Our measurements show that once the sugar is in the phloem it generates high enough pressures to be transported throughout the plant, even in the face of midday water stress. But the question remains: are the observed concentrations too high to allow for diffusion from the photosynthetic cells? *Quercus rubra* has been posited as being a passive loader because of the large quantity of plasmodesmatal pores throughout the pre-phloem pathway, and the lack of sucrose accumulation in veins in ^{14}C autoradiograph studies (Rennie & Turgeon, 2009), but other oak species have been suggested to not be exclusively passive loaders (Öner-Sieben & Lohaus, 2014). If passive loading is occurring, cytoplasmic sucrose concentrations would need to be > 1560 mM for estimates based on 35% of pixels and > 1100 mM for estimates based on all pixels. Based on known bulk leaf sugar concentration (110 mM at midday; Gersony *et al.*, 2020), this seems unlikely given that such levels could only be reached if sucrose is restricted to the cytoplasm (e.g. excluded from the vacuole) and the cytoplasm makes up *c.* < 10% of leaf volume (calculations detailed in Notes S1), neither of which has been found in another oak species (Öner-Sieben & Lohaus, 2014). Furthermore, because bulk leaf osmolality is *c.* 935 mM at midday (Gersony *et al.*, 2020), some cells would need to have a much lower osmolality to balance out the osmolality of the cells with high cytoplasmic sucrose concentrations that are involved in passive loading. Such cellular-level discrepancies in osmolality have not been observed in plasmolysis studies (Russin & Evert, 1985). In sum, the results presented here, for both the conservative estimate and the estimate of sucrose concentration based on the 35% of pixels with the highest concentration, suggest that passive loading is likely not the mechanism by which sucrose is transported into the phloem of mature red oak trees.

Yet, if red oaks are utilizing an active or mixed loading strategy, instead of a purely passive loading strategy, how could there be so many plasmodesmata connecting the mesophyll to the sieve-element companion cell complex, and why

are no veins observed in ^{14}C autoradiograph leaf disc assays for red oak leaves (Rennie & Turgeon, 2009)? Evidence that plasmodesmata can be gated when there are pressure differences between cells of 0.2 MPa may help reconcile these observations (Oparka & Prior, 1992; Park *et al.*, 2019). Certainly, the idea that plasmodesmata may not always be open complicates interpretation of plasmodesmata frequency and ^{14}C autoradiographs with regard to sucrose movement. Furthermore, other studies have suggested that high plasmodesmatal frequency does not prevent active loading (Öner-Sieben & Lohaus, 2014) and that interpretations of ^{14}C autoradiograph studies for trees are complicated due to thicker leaf structure and thicker cuticles (Goggin *et al.*, 2001). Further work is needed to reconcile high sieve element sucrose concentrations with plasmodesmata frequency and dynamics.

Our study describes a novel method for the investigation of phloem functioning. Future work to better understand the wide-reaching applications of this method should include performing this method on species where it is possible to obtain independent measurements of phloem sucrose concentration and performing this method on a wide range of species to understand the effects of varying chemistry. In addition to presenting a new method, this study supports the Münch hypothesis and challenges passive loading for red oak trees. More broadly, these findings will help inform our understanding of ecological processes in the context of global change that are linked to phloem turgor (McDowell *et al.*, 2013; Nikinmaa *et al.*, 2013; Sevanto *et al.*, 2014). By quantifying the previously unknown phloem source dynamics of trees and calculating that the safety-margin for turgor loss in the source phloem is substantial, this study informs our ability to determine factors limiting productivity of trees now and in future climate scenarios.

Author contributions

JTG, AM, and NMH designed the experiment. JTG performed the Raman data collection and the statistical modelling and analysis, with substantial help in practice and theory from AM. JTG wrote the manuscript with contributions from AM and NMH.

ORCID

Jess T. Gersony https://orcid.org/0000-0003-2619-3851

N. Michele Holbrook (ID) https://orcid.org/0000-0003-3325-5395

Arthur McClelland (ID) https://orcid.org/0000-0003-4798-5954

References

Altangerel N, Ariunbold GO, Gorman C, Alkahtani MH, Borrego EJ, Bohlmeyer D, Hemmer P, Kolomiets MV, Yuan JS, Scully MO. 2017. *In vivo* diagnostics of early abiotic plant stress response via Raman spectroscopy. *Proceedings of the National Academy of Sciences, USA* **114**: 3393–3396.

Asner GP, Scurlock JM, Hicke AJ. 2003. Global synthesis of leaf area index observations: implications for ecological and remote sensing studies. *Global Ecology and Biogeography* **12**: 191–205.

Bearce BC, Kohl HC. 1970. Measuring osmotic pressure of sap within live cells by means of a visual melting point apparatus. *Plant Physiology* **46**: 515–519.

Fink D, Dobbelstein E, Barbian A, Lohaus G. 2018. Ratio of sugar concentrations in the phloem sap and the cytosol of mesophyll cells in different tree species as an indicator of the phloem loading mechanism. *Planta* **248**: 661–673.

Gersony JT, Hochberg U, Rockwell FE, Park M, Gauthier PP, Holbrook NM. 2020. Leaf carbon export and nonstructural carbohydrates in relation to diurnal water dynamics in mature oak trees. *Plant Physiology* **183**: 1612–1621.

Gierlinger N, Schwanninger M. 2006. Chemical imaging of poplar wood cell walls by confocal Raman microscopy. *Plant Physiology* **140**: 1246–1254.

Goggin FL, Medville R, Turgeon R. 2001. Phloem loading in the tulip tree. Mechanisms and evolutionary implications. *Plant Physiology* **125**: 891–899.

Guendel A, Rolletschek H, Wagner S, Muszynska A, Borisjuk L. 2018. Micro imaging displays the sucrose landscape within and along its allocation pathways. *Plant Physiology* **178**: 1448–1460.

Hölttä T, Vesala T, Sevanto S, Perämäki M, Nikinmaa E. 2006. Modeling xylem and phloem water flows in trees according to cohesion theory and Münch hypothesis. *Trees* **20**: 67–78.

Jensen KH, Savage JA, Holbrook NM. 2013. Optimal concentration for sugar transport in plants. *Journal of the Royal Society Interface* **10**: 20130055.

Leardi R, González AL. 1998. Genetic algorithms applied to feature selection in PLS regression: how and when to use them. *Chemometrics and Intelligent Laboratory Systems* **41**: 195–207.

Liesche J. 2017. Sucrose transporters and plasmodesmal regulation in passive phloem loading. *Journal of Integrative Plant Biology* **59**: 311–321.

Liesche J, Gao C, Binczycki P, Andersen SR, Rademaker H, Schulz A, Martens HJ. 2019. Direct comparison of leaf plasmodesma structure and function in relation to phloem-loading type. *Plant Physiology* **179**: 1768–1778.

Mandrile L, Rotunno S, Miozzi L, Vaira AM, Giovannozzi AM, Rossi AM, Noris E. 2019. Nondestructive Raman spectroscopy as a tool for early detection and discrimination of the infection of tomato plants by two economically important viruses. *Analytical Chemistry* **91**: 9025–9031.

McDowell NG, Fisher RA, Xu C, Domec Jc, Hölttä T, Mackay DS, Sperry JS, Boutz A, Dickman L, Gehres N *et al.* 2013. Evaluating theories of drought-induced vegetation mortality using a multimodel–experiment framework. *New Phytologist* **200**: 304–321.

Michel BE. 1972. Solute potentials of sucrose solutions. *Plant Physiology* **50**: 196–198.

Munch E. 1930. *Stoffbewegungen in der pflanze*. Jena, Germany: Gustav Fischer.

Nikinmaa E, Hölttä T, Hari P, Kolari P, Mäkelä A, Sevanto S, Vesala T. 2013. Assimilate transport in phloem sets conditions for leaf gas exchange. *Plant, Cell & Environment* **36**: 655–669.

Nikinmaa E, Sievänen R, Hölttä T. 2014. Dynamics of leaf gas exchange, xylem and phloem transport, water potential and carbohydrate concentration in a realistic 3-D model tree crown. *Annals of Botany* **114**: 653–666.

Öner-Sieben S, Lohaus G. 2014. Apoplastic and symplastic phloem loading in *Quercus robur* and *Fraxinus excelsior*. *Journal of Experimental Botany* **65**: 1905–1916.

Oparka KJ, Prior DAM. 1992. Direct evidence for pressure-generated closure of plasmodesmata. *The Plant Journal* **2**: 741–750.

Park K, Knoblauch J, Oparka K, Jensen KH. 2019. Controlling intercellular flow through mechanosensitive plasmodesmata nanopores. *Nature Communications* **10**: 1–7.

Pate JS. 1976. *Transport and transfer processes in plants*. London, UK: Academic Press.

Raschke K. 1979. Movements of stomata. *Encyclopedia of Plant Physiology* **7**: 383–441.

Rennie EA, Turgeon R. 2009. A comprehensive picture of phloem loading strategies. *Proceedings of the National Academy of Sciences, USA* **106**: 14162–14167.

Russin WA, Evert RF. 1985. Studies on the leaf of *Populus deltoides* (Salicaceae): ultrastructure, plasmodesmatal frequency, and solute concentrations. *American Journal of Botany* **72**: 1232–1247.

Savage JA, Beecher SD, Clerx L, Gersony JT, Knoblauch J, Losada JM, Jensen KH, Knoblauch M, Holbrook NM. 2017. Maintenance of carbohydrate transport in tall trees. *Nature Plants* **3**: 965–972.

Sevanto S, Mcdowell NG, Dickman LT, Pangle R, Pockman WT. 2014. How do trees die? A test of the hydraulic failure and carbon starvation hypotheses. *Plant, Cell & Environment* **37**: 153–161.

Slewinski TL, Zhang C, Turgeon R. 2013. Structural and functional heterogeneity in phloem loading and transport. *Frontiers in Plant Science* **4**: 244.

Sokal RR, Rohlf FJ. 1981. *Biometry*. San Francisco, CA, USA: WH Freeman & Co.

Taylor BN, Patterson AE, Ajayi M, Arkebauer R, Bao K, Bray N, Elliott RM, Gauthier PP, Gersony J, Gibson R *et al.* 2017. Growth and physiology of a dominant understory shrub, *Hamamelis virginiana*, following canopy disturbance in a temperate hardwood forest. *Canadian Journal of Forest Research* **47**: 193–202.

Turgeon R, Medville R. 1998. The absence of phloem loading in willow leaves. *Proceedings of the National Academy of Sciences, USA* **95**: 12055–12060.

Supporting Information

Additional Supporting Information may be found online in the Supporting Information section at the end of the article.

Fig. S1 Representative Raman maps of sections of *Quercus rubra* petioles.

Fig. S2 Histograms of all estimated concentrations for each pixel for each *Quercus rubra* leaf, excluding outliers.

Notes S1 Compartmentalization calculations and sucrose concentration estimates for non-sieve element cells.

Table S1 Diameters of sieve elements from the literature.

Table S2 Coefficients of variation for within and between calibration droplets.

Table S3 Percentage of sieve element area in the total phloem area.

Table S4 Comparisons between our findings and the literature.

Please note: Wiley Blackwell are not responsible for the content or functionality of any Supporting Information supplied by the authors. Any queries (other than missing material) should be directed to the *New Phytologist* Central Office.